Micromechanically based integrated optic modulators and switches

Young W. Kim, Mark G. Allen , and Nile F. Hartman*

School of Electrical Engineering
Georgia Institute of Technology
Atlanta, Georgia 30332-0250

* Physical Sciences Laboratory
Georgia Tech Research Institute
Georgia Institute of Technology
Atlanta, Georgia 30332

ABSTRACT

The integration of micromachined devices into integrated optic systems offers the potential for both miniaturization and improved performance of these systems. In this paper, an electromechanical switch integrated with an optical waveguide is described that is suitable for phase and intensity modulation and thus modulation or switching functions. The electromechanical switch is fabricated using surface micromachining techniques and consists of a multilevel polyimide platform, some regions of which are suspended 2-3 μm above the waveguide surface and other region 15 μm above the waveguide surface. The platform is free to move in the vertical direction. Application of voltage between the platform and substrate brings the platform into intimate contact with the waveguide, thus changing the waveguide transmission characteristics. Extensions of this technique to multiple platforms in series to create multibit digital modulation is easily envisioned.

1. INTRODUCTION

Recent developments in micromachining have led to success in building new types of microactuators[1-5]. In addition, the integration of micromechanical components and electrooptic devices onto a silicon wafer or waveguide substrate is currently of great interest, particularly for optical communication applications[6-7]. Some integrated optics applications especially involve switches and modulators; for example, multiplexing/demultiplexing of optical signals, optical beam steering, reconfigurable interconnect, and switch selectable time delay networks[8-12]. To achieve these devices, it is possible to use materials like electooptic materials, e.g. $LiNbO_3$, acoustooptic materials, and ferroelectric liquid crystals. However, it would be also desirable to use passive materials. Advantages of passive materials in integrated optics applications are low loss, lower index of refraction, compatibility with fiber optics, and the ability to be fabricated using standard integrated circuit materials, for example, Si, SiO_2, and Si_3N_4. Thus, it is possible to imagine integrating optical components with electronics. However, the disadvantage of passive materials is that the required change of index must be induced externally. Therefore, we need some mechanical or other perturbation of waveguide materials in order to induce modulation. We realized surface micromachining can be used in high performance optical devices. These devices are useful for optical switches and modulators. Our micromachined fabrication technique allows the actuation of a movable platform and inclusion of electrodes to tune as well as adjust the alignment. The movable platforms can be fabricated on the thin film waveguide on quartz and Si wafers[13]. This paper discusses materials issues that involved in selecting materials for switches and modulators and design considerations which are being developed for several kinds of organic materials and microactuator design and fabrication. Although these devices are being developed particularly for optoelectronics, the fabrication technique can be also applied in other devices, for example microwave components, on waveguide substrates.

2. DEVICE CONCEPT

Integrated optical waveguide switching elements are typically based on materials systems exhibiting electrooptic or accoustooptic properties. In the case of passive waveguide materials systems other approaches must be utilized to achieve switching or modulation functions. These approaches typically rely on surface elements that interact with a guided beam through evanescent effects or by spoiling the waveguiding action. Surface stabilized ferroelectric liquid crystals have been

used to demonstrate a waveguide directional coupler [8] and mechanical rely on the use of surface elements that interact devices. Mechanically based devices have also been reported [9]. The device reported herein is a microactuator based structure used to spoil the optical waveguiding action. Operation is dependent on a moveable platform with a thick dielectric film that makes contact with the waveguide surface.

Upon contact, light is coupled from the waveguide into the platform mounted dielectric film where it is either absorbed or scattered. To promote coupling, the refractive index of the dielectric film must be greater than the waveguide effective refractive index (see Figure 1). Another material issue is that high dissipation in the film may be required to spoil the waveguiding, and to reduce the worry about any light coupled back into waveguide. In addition, the film should be compatible with micromachining techniques so that we can, for example, pattern the material using standard plasma etching. Thus, a variety of material of polyimides and filled polyimides were investigated. We looked into two different types of materials; first, lower-loss materials (Du Pont PI-2555, PI-2611), Second, higher-loss materials such as photosensitive polyimide(Du Pont PI-2721), Probimide 348(Ciba-Geigy), PI-2555(Du Pont) loaded with 10 % carbon black, and PI-2555(Du Pont) loaded with 10 % ferro black.

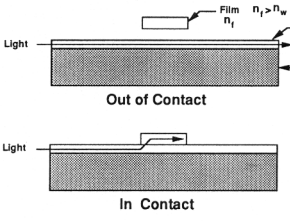

Figure 1. Device concept of attenuator/switch

3. WAVEGUIDE FABRICATION

The optical waveguides are fabricated using an ion exchange process. A borosilicate glass, BK-7, is used as the substrate material due to its excellent optical properties. To generate a waveguide, the glass substrates are immersed in a 0.25 molar % silver nitrate melt buffered with sodium nitrate. For single mode waveguides, a diffusion temperature of approximately 325 °C and an immersion time of 10 minutes is satisfactory. In the as diffused state the substrates will not guide; therefore the waveguide is further annealed an additional 30 minutes at a temperature of 500 °C. The annealing step promotes further diffusion and helps to dissipate any metallic agglomeration. The resulting waveguides are of excellent quality with attenuations of only 0.1 to 0.2 dB/cm at 632.8 nanometers.

4. MATERIALS TESTING

As a test vehicle for the fabrication of a waveguide on ion-exchanged BK-7 glass substrate, a simple channel waveguide was designed and patterned by using a lift-off process to define the waveguide edges. Figure 2 is a photomicrograph of the fabricated channel waveguides. In order to test light transmission as a function of film type for several kinds of polyimides, we prepared two different classes of materials. First, lower loss materials, Du Pont polyimides PI-2555 and PI-2611, were used as received. These materials are slightly yellowish and transparent (note that they are not low loss in the sense of waveguide materials, but they have low loss in comparison to the other materials tested here). Second, higher loss materials such as Du Pont photosensitive polyimide PI-2721, Ciba-Geigy photosensitive polyimide Probimide-348, PI-2555 loaded with carbon black, and PI-2555 loaded with ferro black, were investigated. These latter four materials are translucent or opaque black.

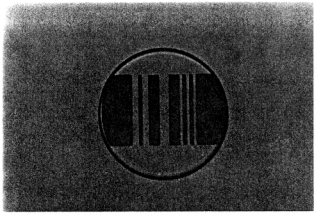

Figure 2. Photomicrograph of waveguide on ion-exchanged BK-7 glass substrate

We prepared two thin films from each of these materials. One had a length of 2.5 mm and the other had a length of 7.5 mm. Both had a thickness of 3 μm. The transmitted light can be measured as a function of incident light intensity with films both in contact and out of contact with the waveguide surface. Our experimental apparatus to accomplish this is shown in Figure 3. Figure 4 shows the experimental arrangement of the microactuator on the waveguide. In Figure 4, P-coupling prism, M-mirror, WG-waveguide, S-substrate, DET-detector, L-lens, MP-movable platform, and EL-electrode. A He-Ne laser (λ=632.8 nm) of 300mW output power was used as the incident light source. The incident laser beam is coupled to the waveguide through a $\lambda/2$ plate filter, so that the incident light intensity reaching the waveguide can be varied. The platform on the top of this waveguide can be electrostatically drawn down to the waveguide surface, thus modifying the waveguide transmission characteristics. For these film studies, the thin films of various materials were used in place of the platform to evaluate their attenuation characteristics prior to platform fabrication.

Figure 5 shows experimental data for lower loss materials. The y-axis is the measured output power of the transmitted light in mW as a function of the input power in mW. The various lower loss materials are plotted together on the same scale; the slope of the data is inversely related to the attenuation characteristics (small slope = large attenuation). A PI-2611 sample which is 2.5 mm in length shows almost no attenuation in this test. If we increase the length of the PI-2611 sample from 2.5 mm to 7.5 mm, we find that the attenuation greatly increases. Examining the PI-2555 samples, both the 2.5 mm and 7.5 mm lengths are highly attenuating. Figure 6 shows experimental data for the higher loss materials. Note that the y-axis ranges from 0 to 30 mW whereas x-axis still ranges from 0 to 300 mW; thus, these attenuations will be larger than for the lower loss materials. Examining these data, the attenuation of the PI-2721 is the least, followed by Ciba-Geigy Probimide-348 and the filled PI-2555 and PI-2611 materials.

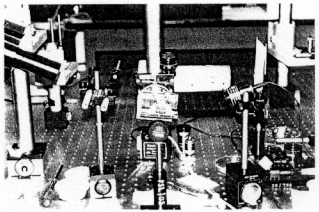

Figure 3. Photograph of experimental apparatus

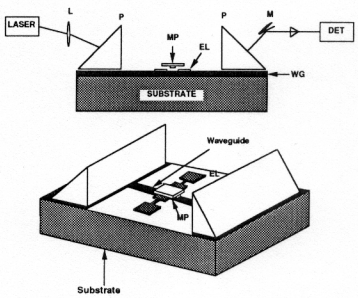

Figure 4. Schematic experimental arrangement of the microactuator on the waveguide

Taking the slope of these lines as a quantitative measure of the attenuation, we can summarize the data we have obtained in Figure 7. Here is shown on the x-axis the different types of materials and for each group the left hand bar represents 2.5 mm length of film covering the waveguide, and the right hand bar represents the 7.5 mm length film covering the waveguide. There are several results which can be immediately extracted from these data. First, the 2.5 mm film always has less attenuation than the 7.5 mm film; i.e., the more film area in contact with waveguide, the larger the attenuation losses. Second, the relative performance of these materials is assessed. We find that PI-2555 loaded with 10% ferro black and PI-2555 loaded with 10% carbon black performed relatively well, whereas the other materials are relatively poor in terms of their attenuation. The ferro black material, however, could not be plasma-patterned since the ferro black dye used with not plasma etchable; however, the carbon black polyimide and PI-2555 could be plasma etched. Therefore, either of these materials are very good candidates for the electrostatically actuated platform attenuator.

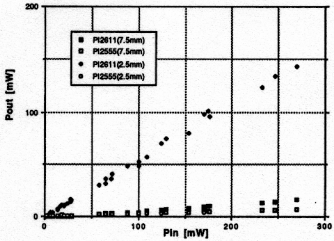

Figure 5. Incident light versus guided output power for lower loss materials

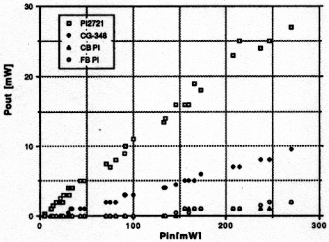

Figure 6. Incident light versus guided output power for higher loss materials

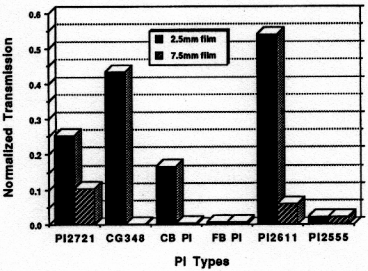

Figure 7. The slope of transmission data for several kinds of polyimides

5. PLATFORM FABRICATION

5.1 Single Layer Surface Micromachined Platforms

Surface micromachined movable platforms are used as the waveguide spoiling element. Typical platform sizes are squares ranging from 50-2000 μm on a side, suspended by four diagonally-oriented arms ranging from 50-2000 μm in length. The structure is fabricated using surface micromachining techniques as shown in Figure 8. An oxidized silicon wafer and an ion-exchanged BK-7 glass substrate are prepared as the starting material. An adhesion layer of chromium 200 Å in thickness followed by a gold layer 3800 Å in thickness is evaporated onto the wafer using an E-beam evaporator and patterned into an electrode pattern for use in electrostatic plate positioning. The wafer and electrodes are then coated with an insulating layer of polyimide (Du Pont PI-2555) deposited in one spin coat of 5000 rpm for 30 seconds, followed by a prebake of 130 °C for 20 minutes in air and a final cure of 300 °C for one hour in air (Figure 8a). Layers of chromium (for adhesion) and copper (as electroplating seed layer) are then deposited as described above and patterned to form anchors for the arms of the movable plate, and additional copper (the sacrificial layer) is electroplated to a final thickness of approximately 15 microns (Figure 8b). A second layer of polyimide (the structural material) with an after-cure thickness of approximately 7.5 microns is deposited. In order to pattern the polyimide, a hard metal mask of 200 Å of chromium (as an adhesion layer)

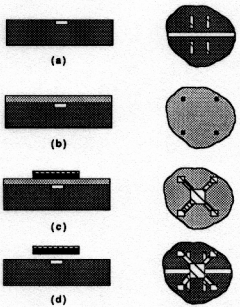

Figure 8. Fabrication sequence of surface micromachined platforms. (a) after deposition of polyimide over patterned electrodes; (b) after electroplating of sacrificial layer; (c) after deposition and patterning of structural polyimide layer; (d) after etch of sacrificial layer.

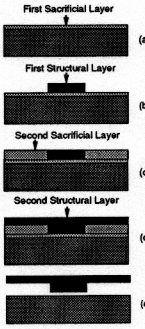

and 2500 Å of gold is evaporated onto the polyimide and patterned to form the platforms using a solution of iodine and potassium iodide in water as the gold etchant. The exposed polyimide is then etched in a 10% CF_4 - 90% O_2 plasma to form the gold-covered polyimide platforms and expose the sacrificial layer (Figure 8c). Finally, the copper sacrificial layer is removed using a ferric chloride etch at room temperature to free the polyimide plates (Figure 8d). The plates typically took 1 - 2 hours to release depending on their size.

5.2 Multilayer and Molded Surface Micromachined Platforms

The structures are fabricated in a similar fashion to the single-layer structures along with the modifications described in Figure 9. A borosilicate glass, BK-7, substrate prepared as described in the section 3 is used as the starting material. An adhesion layer of chromium 200 Å in thickness followed by a gold layer 3800 Å in thickness is evaporated onto the wafer using an electron beam evaporator and patterned into an electrode pattern for use in electrostatic plate positioning. A copper layer approximately 3 μm in thickness (the first sacrificial layer) is then evaporated on the wafer using an electron beam evaporator and patterned to form anchors for the arms of the movable plate. The thickness of this layer could be optionally increased by electroplating, but this was not done for the platforms described here. The first structural layer is then deposited. Du Pont PI-2555 is spin-cast in four coats of 2750 rpm for 90 seconds, with a soft bake of 130 °C for 20 minutes between coats. Upon deposition of the four coats, the polyimide is cured at 300 °C for 60 minutes in air, yielding an after-cure thickness of approximately 12 μm. This polyimide is patterned using 100% oxygen plasma to form the first structural layer. The wafer is then immersed in a copper electroplating solution as described above and the second sacrificial layer is deposited in a self-aligned manner. Deposition is stopped when the second sacrificial layer reaches the top of the first structural layer, yielding a sacrificial layer thickness of 12 μm. A second polyimide layer (second structural layer) is deposited identically to the first structural layer. A hard metal mask of 200 Å of chromium (as an adhesion layer) and 4000 Å of gold is evaporated onto the polyimide and patterned to form the platforms using a solution of iodine and potassium iodide in water as the gold etchant. The exposed polyimide is then etched in a 100% oxygen plasma to form the gold-covered polyimide platforms and expose the sacrificial layer. Finally, the copper sacrificial layer is removed using a ferric chloride etch at room temperature to free the multilayer platforms. These relatively small platforms typically took approximately 1 hour to release. Scanning electron micrographs of the fabricated structures are shown in Figure 10. Figure 10(a) is a top view of the fabricated structure, which Figure 10(b) is an angular view. The multilayer aspect of the platform is evident in the angular view. The arms of the platform are suspended 15 μm above the surface, which the lowest part of the platform is only 3 μm above the surface.

Figure 9. Schematic representation of multilayer platform fabrication. The sacrificial layer is shown in light shade while the bridge material is shown in black. (a) after deposition of first sacrificial layer; (b) after deposition and patterning of first structural material; (c) after selective deposition of second sacrificial layer; (d) after deposition and patterning of second structural material; (e) after removal of sacrificial layer.

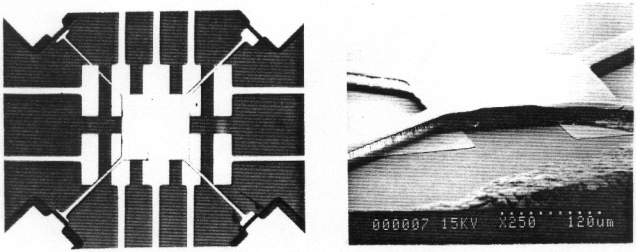

(a) (b)

Figure 10. Scanning electron micrographs of multilayer surface micromachined platform. (a) Top view; (b) side view. The upper platform is approximately 400 μm on a side, and is suspended by arms approximately 500 μm long, 40 μm wide, and 12 μm thick. The lower platform is approximately 400 μm long, 70 μm wide, and 12 μm thick, and is integrally attached to the upper platform. The lower platform is suspended approximately 3 μm above the surface, while the upper platform is suspended approximately 15 μm above the surface.

In order to get good contact and light absorption structures, molded surface micromachined movable platforms were fabricated. The structures are fabricated in a similar fashion to multilayer structures in the above. After depositing the first sacrificial layer, it covers with cured-photoresist as a molding pattern (instead of polyimide) and electroplated sacrificial layer.

6. ELECTROSTATIC RESULTS

In single layer surface micromachined platforms, we have mechanically deflected the largest plate as much as three hundred microns in the plane of the wafer, and 15 microns normal to the plane of the wafer. The qualitative electrostatic actuation of these devices was also investigated, and successful actuation was achieved. For example, for a 100 x 100 μm square platform suspended 15 μm from the surface of the wafer, application of 50 V between the platform was sufficient to attract the plate 15 μm down to the surface.

In multilayer surface micromachined platforms, application of approximately 65 volts between the platform and an electrode laterally displaced on the surface was sufficient to laterally deflect the platform approximately 5 μm. This structure will be useful in optomechanical applications currently under investigation where intimate contact between platform and substrate is necessary with no intervening electrostatic electrodes shielding or otherwise interfering with the contact. Thus, this process can be used to fabricate electrostatically actuatable structures suspended several tens of microns above the surface of the wafer. However, only small changes in transmitted light were observed upon actuation. Performance is much less than expected from film studies. We are currently investigating dirt/contamination, achieving good contact, and processing residues between polyimide and waveguide.

7. CONCLUSIONS

In summary, we have proposed devices for achieving IO modulators and switches on passive waveguide structures and demonstrated the concept using polyimide and filled polyimide films. Also, the technology for the microfabrication of platforms and their combination with optical waveguide structures have been demonstrated.

8. ACKNOWLEDGMENTS

This work is partially supported by the National Science Foundation under grant ECS-9117074. Microfabrication described in this work was carried out in the Georgia Tech Microelectronics Research Center (MiRC). The authors would also like to thank MSMA(microsensors and microactuators) group members and Ms. Linda Lin of Georgia Tech for assistance with measuring refractive indices that appear in this work. Finally, the authors wish to thank Du Pont for the donation of the polyimides used in this work.

9. REFERENCES

1. R.T. Howe and R.S. Muller, "Polycrystalline Silicon Micromechanical Beams", J. Electrochem. Soc., vol.130, 1983, p.1420.

2. M.A. Schmidt, R.T. Howe, S.D. Senturia, and J.H.Haritonidis, "Design and Calibration of a Microfabricated Floating Element Shear-Stress Sensor", IEEE Trans. on Electron Devices, vol. 35, no. 6, 1988, pp. 750-757.

3. L.S. Fan, Y.C. Tai, and R.S. Muller, "IC-processed Electrostatic Micromotors", Proceedings of the 1988 IEEE International Electron Devices Meeting, San Francisco, CA, December 1988, pp. 666-669.

4. W.C. Tang, R.T. Howe, "Electrostatic Comb Driver of Lateral Polysilicion Resonators", Sensors and Actuators, A21-A23, 1990, pp. 328-331.

5. J.P. Cummings, R.J. Jensen, D.J. Kompelien, and T.J. Moravec, "Technology Base for High Performance Packaging", Proceedings of the Electronic Components Conference, 1982, pp. 465-478.

6. C. Liao and G.I. Stegeman, "Nonlinear prism coupler," Appl. Phys. Lett. Vol.44(2),pp164-166, Jan. 1984.

7. H. Bezzaoui and E. Voges, "Integrated optics combined with micromechanics on silicon," Sensors and Actuators A29, pp219-223, 1991.

8. Clark, N. A., Handschy, M. A., "Surface-stabilized ferroelectro liquid-crystal electro-optic waveguide switch", Applied Physics Letters, 57 (18) 29 October 1990.

9. Hemmi, C., Takle, C., "Optically controlled phased array beamforming using time delay", 2nd Annual DARP/Rome Laboratory Symposium on Photonic Systems for Antenna Applications, PSAA-91, 10-12 December 1991, Monterey, California.

10. Hartman, N.F., Corey, L.E., "A New Integrated Optic Technique for Time Delays in Wideband Phase Arrays", IEEE Conference Publication No.333, Seventh International Conference of Antennas and Propagation (ICAP 91), University of York, York, U.K., April 15-18, 1991.

11. Hartman, N.F., Corey, L.E., "A New Time Delay Concept Using Integrated Optic Technique", International IEEE AP-S Symposium, June 24-28, 1991, The University of Western Ontario, London Ontario, Canada.

12. C. Camperi-Ginestet, Y.W. Kim, N.M. Jokerst, M.G. Allen, and M.A. Brooke, "Vertical Electrical Interconnection of Component Semiconductor Thin-Film Devices to Underlying Silicon Circuitry," IEEE Photon. Technol. Letter., Vol.4, No.9, pp1003-1006.

13. Young W. Kim and Mark G. Allen, "Single and Multilayer Surface micromachined Platforms Using Electroplated Sacrificial Layers," Sensors and Actuators A, Vol.35, No.1, pp61-68, 1993.